Published in final edited form as:
Cell Rep. 2014 June 12; 7(5): 1716–1728. doi:10.1016/j.celrep.2014.04.031.

Impact of regulated secretion on anti-parasitic CD8 T cell responses

Harshita Satija Grover[1,#], **H. Hamlet Chu**[1,#], **Felice D. Kelly**[2], **Soo Jung Yang**[1], **Michael L. Reese**[2,%], **Nicolas Blanchard**[3], **Federico Gonzalez**[1], **Shiao Wei Chan**[1], **John C. Boothroyd**[2], **Nilabh Shastri**[1,*], and **Ellen A. Robey**[1,*]

[1]Division of Immunology and Pathogenesis, Department of Molecular and Cellular Biology, University of California, Berkeley, CA 94720-3200

[2]Department of Microbiology and Immunology, Stanford University School of Medicine, Stanford, CA 94305-5124.

[3]Center of Pathophysiology of Toulouse-Purpan, INSERM UMR1043 - CNRS UMR5282 – University of Toulouse, 31024 Toulouse Cedex 3, France.

Summary

CD8 T cells play a key role in defense against the intracellular parasite *Toxoplasma* but why certain CD8 responses are more potent than others is not well understood. Here, we describe a parasite antigen ROP5 that elicits a modest CD8 T cell response in genetically susceptible mice. ROP5 is secreted via parasite organelles termed rhoptries that are injected directly into host cells during invasion, whereas the protective, dense granule antigen, GRA6, is constitutively secreted into the parasitophorous vacuole. Transgenic parasites in which the ROP5 antigenic epitope was targeted for secretion through dense granules led to enhanced CD8 T cell responses, whereas targeting the GRA6 epitope to rhoptries led to reduced CD8 responses. CD8 T cell responses to the dense granule-targeted ROP5 epitope resulted in reduced parasite load in the brain. These data suggest that the mode of secretion impacts the efficacy of parasite-specific CD8 T cell responses.

Introduction

CD8 T cells are key for the control of intracellular pathogens, including the protozoan parasite *Toxoplasma gondii (T. gondii). T. gondii* infects a wide array of warm-blooded hosts, including one third of humans worldwide (Carruthers, 2002; Montoya and Liesenfeld, 2004), but typically causes little pathology, due in part to a robust T cell response (Brown

[*]Address correspondence to Dr. Ellen Robey or Dr. Nilabh Shastri: Mailing Address: 142 Life Sciences Addition #3200, Department of Molecular and Cell Biology, Division of Immunology and Pathogenesis, University of California, Berkeley, CA 94720-3200. Ellen Robey: Phone: (510) 642-8669. Fax: (510) 643-9500. erobey@berkeley.edu. Nilabh Shastri: Phone: (510) 643-9197. Fax: (510) 643-9230. nshastri@berkeley.edu..
[#]co-first authors
[%]current address: Dept. of Pharmacology, University of Texas, Southwestern Medical Center, Dallas, TX 75390-9003

and McLeod, 1990; Denkers and Gazzinelli, 1998; Hakim et al., 1991; Lindberg and Frenkel, 1977). However, not all CD8 T cell responses are equally effective in controlling the parasite, as dramatically illustrated by the differential sensitivity to infection in two inbred mouse strains, BALB/c and C57BL/6 (B6). BALB/c mice show strong resistance to infection due to the presence of the protective MHC class I allele H-2L^{d}, whereas B6 mice, which lack this particular allele, are highly sensitive (Brown et al., 1995; Brown and McLeod, 1990; Suzuki et al., 1994; Suzuki et al., 1991). We recently showed that the protective effect of MHC class I H-2L^{d} is due to a potent CD8 T cell response directed against a single parasite protein, GRA6 (Blanchard et al., 2008). H-2L^{d}-GRA6 -specific T cells account for the majority of CD8 T cells in the brains of infected H-2^{d} mice and effectively control parasite load. In contrast, B6 (H-2^{b}) mice exhibit much higher parasite loads in the brain and eventually succumb to infection, despite the presence of parasite-specific CD8 T cells (Schaeffer et al., 2009). Understanding why particular CD8 T cell responses predominate over others, and why some responses provide more effective protection is critical to designing improved vaccines and other therapies to intracellular pathogens.

One factor that may influence the immunogenicity and immunoprotection of potential CD8 antigens is the intracellular pathway by which pathogen-derived antigens are processed and presented in infected host cells. For cytosolic antigens, such as many viral antigens, presentation is via the classical class I MHC presentation pathway. In this pathway, proteins are degraded in the host cytosol by proteasomes and the resulting peptides are transported into the ER via the TAP transporter, receive a final trimming by the ERRAP, are loaded onto MHC class I, and finally are transported to the surface as peptide-MHC complexes for recognition by a CD8 T cell. In contrast, for pathogen proteins that enter the cell via phagocytosis, antigen presentation occurs by an alternative “cross-presentation” pathway requiring an additional phagosome to ER vesicular transport step (Joffre et al., 2012). The importance of antigen compartmentalization for the CD8 T cell response is illustrated by the protective response to intracellular bacteria when the antigen is secreted into the cytosol, but not when the antigen is retained inside the bacteria (Shen et al., 1998).

For intracellular parasites, the pathways by which potential antigens traffic from the pathogen into the host cell may also impact CD8 T cell responses. For example, *T. gondii* resides within a specialized non-fusogenic compartment, the parasitophorous vacuole that restricts the movement of material into the host cytosol and thus poses a barrier to antigen presentation. Nevertheless, studies with model antigens have shown that proteins that are constitutively secreted into the parasitophorous vacuole lumen via parasite organelles termed dense granules can elicit strong CD8 T cell responses (Gregg et al., 2011; Gubbels et al., 2005). Moreover, the potent endogenous CD8 antigen GRA6 is also constitutively secreted via dense granules (Blanchard et al., 2008). *Toxoplasma* also possesses distinct secretory organelles termed rhoptries that are injected directly into the host cell during productive and abortive invasion events (Blader and Saeij, 2009; Boothroyd and Dubremetz, 2008; Koshy et al., 2012), and this distinct spatial and temporal pattern of secretion could affect the ability of a parasite protein to be presented by MHC class I. All endogenous *T. gondii* CD8 antigens identified to date possess secretory signals, and include both dense

granule and rhoptry proteins (Frickel et al., 2008; Wilson et al., 2010) Blanchard et al., 2008). How the mode of secretion of potential *T. gondii* antigens affects the nature of the CD8 T cell response however, has not been investigated.

A comparison between the immunodominant, protective H-2L^{d}-GRA6 response versus the endogenous T cell response from susceptible H-2^{b} mice should reveal clues about what makes an optimal CD8 T cell response. Aside from GRA6, all other defined endogenous MHC-I restricted *T. gondii* antigens have been identified using prediction strategies (Frickel et al., 2008; Khan et al., 1994; Khan et al., 1988; Wilson et al., 2010). These approaches, while useful, may miss many endogenous responses that do not fit into a given set of assumptions. In contrast, the alternative approach of using T cells from infected mice to probe expression libraries provides a relatively unbiased approach to characterizing endogenous T cell responses (Blanchard et al., 2008; Malarkannan et al., 2001).

Here we used an expression-cloning approach to characterize the CD8 T cell response in H-2^{b} mice, leading to the identification of a nonamer peptide, YAL9, derived from the rhoptry-targeted parasite protein ROP5. In comparison to the H-2L^{d}-GRA6 response, the H-2D^{b}-ROP5 (YAL9) response makes up a relatively small proportion of the endogenous CD8 T cell response to the parasite and does not confer strong protection. To test the impact of regulated secretion on the T cell response, we engineered parasites in which the YAL9 epitope from ROP5 was altered from its normal rhoptry targeting to secretion via dense granules, and we examined the impact of this alteration on the T cell response. Redirecting the ROP5 epitope to the dense granules led to a dramatic increase in the number and protective capacity of H-2D^{b}-ROP5-specific T cells and to a reduced cyst burden in chronically infected mice. Conversely, retargeting the T cell-stimulatory epitope from GRA6 (HF10) for secretion via rhoptries led to a substantially reduced T cell response. Our data suggest that the mode of protein secretion can have a dramatic effect on the magnitude and efficacy of the CD8 T cell response, with important implications for immunity to *T. gondii* and related malarial causing intracellular parasites.

Results

T. gondii immunized C57BL/6 mice elicits potent CD4 but weaker CD8 T cell responses

To characterize the T cell response in the C57BL/6 (B6, H-2^{b}) mice, we immunized animals with irradiated tachyzoites of the type II *T. gondii* strain, *Prugniaud* (Pru) and examined *T. gondii*-specific CD4 and CD8 T cell responses *ex-vivo* at 2 weeks. In contrast to H-2^{d} mice, in which the CD8 T cell response dominates over the CD4 T cell response (Blanchard et al., 2008), B6 mice generated a robust CD4 T cell response but a weaker CD8 response towards *T. gondii* (Figure 1A, top panels; (Grover et al., 2012). To selectively expand the CD8 T cells, we used MHC Class II deficient dendritic cells as APCs for *in vitro* restimulations. The *T. gondii*-specific CD8 T cells progressively expanded over successive *in vitro* restimulation cultures (Figures 1A, lower panels and 1B-C).

Generation of a *T. gondii*-specific CD8 T cell hybridoma

To further characterize *T. gondii*-specific CD8 T cell response at a clonal level we generated *T. gondii*-specific lacZ-inducible CD8 T cell hybridomas as described previously (Karttunen et al., 1992; Sanderson and Shastri, 1994). One such hybridoma, referred to as BTg45Z, produced lacZ when co-cultured with BMDC infected with *T. gondii* (Figure 1D) and this response was blocked by anti-H-2D^b but not anti-H-2K^b monoclonal antibody. Thus, the BTg45Z hybridoma was *T. gondii*-specific and restricted by the H-2D^b MHC class I molecule.

ROP5 is the antigenic protein recognized by CD8 T cell hybridoma

We identified the *T. gondii* antigenic protein by expression cloning. A *T. gondii*-derived cDNA expression library was screened for BTg45Z stimulating genes (Figure S1) (Blanchard et al., 2008). APCs transfected with two cDNA pools (pTg8E6 and pTg13B7) stimulated the BTg45Z T cell hybrid (Figure 2A). Fractionation of the cDNA pools yielded an antigenic active clone pTg8E6.1 (Figure 2B) that encoded a member of the rhoptry protein 5 (ROP5) family of proteins. The ROP5 locus is located on chromosome XII, and encodes a polymorphic family of 4-10 pseudokinases that differ both between *Toxoplasma* strains and between individual genes within a single cluster (Reese et al., 2011). Sequence comparison with different polymorphic versions of ROP5 in the type II strain of *T. gondii* (Reese et al., 2011) revealed that pTg8E6.1 matched the ROP5 version IIC, a protein of 549 amino acids (Figure 2C).

Identification of the minimal antigenic peptide

To define the minimal antigenic peptide recognized by the BTg45Z hybrid, we tested candidate peptides predicted to bind D^b MHC (www.immunepitope.org) (Figure 3A). Analysis of cDNA deletion constructs suggested that the antigenic activity mapped to the YAVANYFFL (YAL9) peptide (Figure 3B). Moreover, the YAL9 peptide had higher antigenic activity relative to N-terminally extended versions of the peptide (Figure 3C), and was found in HPLC fractionated extracts of cells transfected with pTg8E6.1 (Figure S1). We conclude that ROP5IIC was processed by APCs to the YAL9 peptide that was presented by MHC I H-2 D^b and recognized by BTg45Z T cells.

Presentation of YAL9 requires proteasome and TAP, and is partially dependent on ERAAP

In the classical MHC Class I presentation pathway, cytosolic proteins are broken down into peptides by the proteasome, and are transported into the ER via TAP. In the ER, some peptides are further processed by the aminopeptidase ERAAP, and loaded on to MHC Class I molecules (Serwold et al., 2001). To assess whether presentation of YAL9 peptide required the components of the classic MHC-I presentation pathway, BMDCs from wild-type B6, TAP-/- or ERAAP-/- mice were infected and used as APCs to stimulate the BTg45Z hybridoma. The BTg45Z cell response was completely abolished in TAP-deficient cells, and strongly inhibited by the proteasome inhibitor lactacystin (Figure S2). In contrast, loss of ERAAP only partially inhibited BTg45z responses. Thus, presentation of YAL9 requires proteasome processing in the cytoplasm and transport by TAP into the ER, but is only partially dependent on further trimming by ERAAP.

Detection of YAL9-specific CD8 T cells in *T. gondii* infected mice

We next assessed the contribution of YAL9-specific CD8 T cells to the overall T cell response to the parasite. We orally infected H-2^b (C57BL/6) mice and determined the abundance of specific T cells in the CD8 T cell repertoire four weeks post-infection by H-2D^b-YAL9 MHC tetramer staining and intracellular cytokine staining (ICCS) after *ex vivo* restimulation with the YAL9 peptide (Figure 4A-E). The YAL9-specific T cells, as measured by ICCS, made up 0.3% of splenic CD8 T cells (Figure 4B). Based on the ~3.5% parasite-specific cells amongst total CD8 T cells, we estimate that ~10% of parasite-specific CD8 splenocytes are specific for YAL9. Tetramer staining gave a slightly higher value (0.5%) of YAL9-specific T cells amongst splenic CD8 T cells, perhaps due to higher sensitivity of this assay (Figure 4C). Amongst CD8 T cells in the brain, YAL9-specific cells made up ~1% of the CD8 response based on both ICCS and tetramer staining, corresponding to ~10% of the total parasite-specific CD8 response as estimated by ICCS (Figure 4D and 4E). Analyses of mice that were immunized with irradiated parasites gave similar results, with ~0.5% of splenic CD8 T cells showing reactivity to the YAL9 peptide (Figure 4F-H). Thus, unlike the response to the GRA6 derived peptide HF10, which dominates the CD8 T cell response to the parasites in H-2^d mice (Blanchard et al., 2008), the ROP5 derived YAL9 peptide is a detectable, but minor component of the CD8 T cell response in H-2^b mice.

Immunization of H-2^d mice with dendritic cells pulsed with the single HF10 peptide derived from the dense granule protein GRA6, elicited robust protection to challenge with live parasites (Blanchard et al., 2008). To determine the protective potential of the YAL9-specific CD8 T cells, we immunized B6 mice with dendritic cells pulsed with YAL9 peptide and challenged the mice with a lethal dose of *T. gondii*. We observed no statistically significant difference in the survival (Figure S3A), cyst number or the parasite load (Figure S3H and S3I) between mice immunized with the YAL9 versus an irrelevant H-2D^b binding peptide. These results are consistent with evidence that the GRA6 response alone can account for the protective effect of MHC-class I H-2L^d expression on an H-2^d background (Brown et al., 1995; Blanchard 2009; Feliu et al., 2013), implying none of the parasite antigens presented by H-2^b class I alleles provide as strong protection as H-2L^d-HF10.

Generation of transgenic parasites with altered intracellular trafficking of T cell epitopes

The ROP5 and GRA6 antigenic precursors differ in their modes of secretion by *T. gondii* (Figure 5A). The ROP5 protein is secreted into host cells during parasite invasion via secretory organelles known as rhoptries, while GRA6 is constitutively secreted into the parasitophorous vacuole through dense granules. To assess the influence of differential protein targeting on T cell responses, we generated three HA- or FLAG-tagged constructs encoding type II ROP5 (the so-called IIC allele) and GRA6 genes, along with constructs designed to swap the secretion patterns of the antigenic ROP5 and GRA6 peptides (Figures 5B and S4). These constructs were: 1) GRA6-YAL9 which replaces the T-cell epitope of GRA6 (HF10) with that of ROP5 (YAL9) to target this normally rhoptry peptide to dense granules; 2) GRA6-ROP5 which has the promoter and signal peptide of the *GRA6* gene (Gendrin et al., 2010) fused upstream of the C-terminal domain of ROP5, including the YAL9 epitope, thus, also targeting the bulk of this rhoptry protein to dense granules; and 3)

ROP5-HF10 in which the HF10 epitope of GRA6 is fused to the C-terminus of ROP5, thus targeting this normally dense granule peptide for secretion via rhoptries.

We introduced these constructs as transgenes into the type III parasite strain, CTG, whose alleles of GRA6 and ROP5 do not encode the YAL9 or HF10 T cell-stimulatory epitopes (Blanchard et al., 2008; Reese et al., 2011; Feliu et al., 2013). To confirm the appropriate targeting of the proteins, we performed immunofluorescence analysis of transgenic parasites (Figure S4B, C). As expected, parasites expressing GRA6, GRA6-YAL9 and GRA6-ROP5 all displayed transgenic protein co-localization with the dense granule marker, GRA7 (Figure S4B, C), whereas parasites expressing ROP5-HF10 displayed accumulation of transgenic protein in structures that co-localized with rhoptry markers ROP2, 3, 4 (Figure S4B). On the other hand, and also as expected, CTG harboring the wild type ROP5 construct showed a typical rhoptry pattern of staining, and failed to localize with GRA7 (Figure S4C). Western blot analysis indicated that GRA6-YAL9 was expressed at somewhat lower levels (~1/3) than what was seen for GRA6-ROP5 (Figure S4D). Comparison of the HA-tagged GRA6-ROP5 and the FLAG-tagged ROP5 indicated that ROP5 was also expressed at a lower level (~1/5 – 1/10) relative to GRA6-ROP5 (Figure S4E). For the parasite strains expressing the GRA6 epitope HF10, ROP5-HF10 levels were similar to transgenic GRA6 (Figure S4F).

Immunogenicity of antigenic peptides is enhanced by targeting the precursor protein to dense granules

We next assessed the ability of transgenic parasites to stimulate ROP5-specific or GRA6-specific T cells. We expected that the parental CTG strain would not elicit a YAL9-specific T cell response since this strain harbors ROP5 alleles that lack this antigenic epitope (Reese et al., 2011). To confirm this, we measured response of the BTg45Z hybridoma to dendritic cells infected with CTG parasites or pulsed with peptides derived from the regions corresponding to the YAL9 peptide in the allelic forms of ROP5 contained within the CTG parasites (Figure S5A-C). As expected, we observed no detectable response to CTG parasites or to these alternate ROP5 peptides. Interestingly, a polymorphic peptide from another type II allele within the multigene ROP5 locus (ROP5IIA, identical to YAL9 except for a L substituting for a F at position 8) stimulated the hybridoma comparably to that seen with YAL9 from ROP5IIC (Figure S5C). However, and as predicted by their respective genome sequences, neither the CTG nor RH parasites strains express a form of ROP5 that stimulates our ROP5 specific hybridoma (data not shown). We also confirmed that immunization of mice with irradiated CTG parasites does not elicit a detectable response to the YAL9 epitope as measured by both ICCS and tetramer staining (Figure S5D and S5E).

To assess whether the immunogenicity of the YAL9 or HF10 epitopes was affected by altering the secretion of the precursor protein, we infected dendritic cells with the transgenic parasites described above and measured peptide presentation using the corresponding lacZ-inducible hybridoma. The ROP5-specific BTg45Z hybridoma response to transgenic CTG parasites expressing either of the dense granule targeted YAL9 constructs (GRA6-ROP5 and GRA6-YAL9) was substantially higher than those expressing YAL9 in its native form, i.e., as a part of ROP5IIC targeted to its normal location, the rhoptries (Figure 5C, left panel). On

the other hand, the GRA6-specific CTgEZ4 hybridoma response to parasites harboring the rhoptry targeted HF10 peptide (ROP5-HF10) was substantially reduced compared to response to the normally dense granule targeted version of the epitope (Figure 5C, right panel).

We compared the different transgenic parasite strains for their ability to elicit CD8 T cell responses *in vivo*. We infected mice and examined T cell responses in spleen and brain leukocytes 3-4 wks post-infection. At day 21 post infection, ROP5-specific T cells made up ~0.5% of the total CD8 T cell population in the spleen and brains of mice infected with type III CTG parasites expressing the normally targeted ROP5 protein, similar to the results with the type II strains, Pru and ME49 (Figure 5D). Strikingly, infection with CTG+GRA6-ROP5 parasites elicited a 10-20× higher YAL9-specific T cell response compared to CTG+ROP5 parasites as measured by tetramer staining (Figure 5D). In spite of the increase in the number of specific T cells in the brain, their expression of effector/memory markers KLRG-1 and IL7R remained unchanged (Figure 5E). In addition, comparison of the YAL9-specific versus parasite-specific CD8 T cells using *in vitro* restimulation and intracellular IFN-γ staining revealed that the YAL9-specific T cell response accounted for the bulk of the anti-parasite CD8 response in mice infected with CTG+GRA6-ROP5 parasites (Figure 5F). This predominance of the YAL9-specific response resulted in a significant decrease in the CD4 to CD8 ratio amongst parasite-specific IFN-γ producing T cells in both the spleen and brain (Figure 5G). The YAL9-specific CD8 T cell response to the CTG+GRA6-YAL9 strain was also enhanced compared to CTG+ROP5, although to a lesser extent than with CTG +GRA6-ROP5 parasites (Figures 5D and 5F-5G). Similar enhancement of the CD8 T cell response to dense granule targeted YAL9 was also observed when mice were immunized with irradiated transgenic parasites (Figure 5H and 5I).

We observed a similar correlation between enhanced T cell response and dense granule targeting with the GRA6 epitope (Figure 5J). GRA6-specific T cells made up ~10% of the total CD8 T cell population in the spleen and 30% in the brains of mice infected with CTG parasites expressing the normally targeted GRA6 protein, similar to the results with the type II strain Pru (Figure 5J). In contrast, mice infected with parasites harboring the rhoptry-targeted version of the GRA6 epitope (ROP5-HF10) had 3-4 fold lower numbers of GRA6-specific T cells. Together these data indicate that the same T cell epitope evokes a greater T cell response when secreted via dense granules versus rhoptries.

YAL9-specific T cells provide protection against parasites in which the epitope is targeted to dense granules

In some settings CD8 T cells may be expanded effectively, but still fail to provide strong protection (Shen et al., 1998). To determine if re-targeting of the YAL9 epitope could enhance immune protection as well as CD8 expansion, we examined the ability of peptide-DC immunization to provide protection against transgenic parasites in which the YAL9-containing protein was targeted for secretion via dense granules versus rhoptries. We performed peptide immunization with YAL9 according to the scheme in Figure 6A, and challenged i.p. with a high dose of CTG+ROP5 or CTG+GRA6-ROP5 transgenic parasites. Strikingly, all of the mice that were immunized with YAL9 and then challenged with CTG

+GRA6-ROP5 survived the acute phase of infection. In contrast, the majority of mice that were immunized with YAL9 peptide and then challenged with CTG+ROP5, or immunized with control peptide (WI9), succumbed to infection within the first week after challenge (Figure 6B). Thus, the combination of peptide immunization to create a pre-existing ROP5-specific T cell population, and challenge with parasites harboring the epitope targeted for secretion via dense granules, provided strong immune protection during the acute phase of infection.

To further explore the mechanism of protection, we measured the T cell responses in the chronic phase of infection in the surviving mice (Figure 6C-E). Interestingly, there was an enhanced YAL9-specific response in the brains of CTG+GRA6-ROP5 infected animals irrespective of the peptide immunization. This difference was seen as an increased proportion of YAL9-specific CD8 T cells based on tetramer staining (Figure 6C), *ex-vivo* restimulation followed by ICCS for IFN-γ (Figure 6D), and an overall decrease in the CD4 to CD8 ratio amongst interferon gamma producing, *T. gondii*-specific T cells (Figure 6E). Similar trends were observed in the splenic T cells of surviving mice (Figure S6A-C). We also observed a marked difference in cyst load of surviving mice chronically infected with CTG+ROP5 relative to CTG+GRA6-ROP5, regardless of the peptide immunization (Figure 6F). This difference is likely due to a more protective CD8 T cell response, rather than reduced overall fitness of parasite strains, since CTG+GRA6-ROP5, CTG+GRA6, and CTG +ROP5 transgenic parasites all displayed similar growth in TAP-/- mice, which lack a functional CD8 T cell response (data not shown). These data indicate the YAL9-specific CD8 T cells generated upon challenge with CTG+GRA6-ROP5 parasites can eventually expand and predominate in the brain and control parasites during the chronic phase of infection, provided that mice can survive the acute phase. Moreover, the generation of pre-existing YAL9-specific T cells by peptide immunization can allow for survival of acute infection, but only when mice are challenged with parasites expressing the dense granule targeted YAL9. These data imply that both superior T cell expansion and superior protection contribute to the efficacy of the CD8 T cell response to dense granule targeted YAL9. Moreover, these results imply that constitutively secreted endogenous parasite antigens provide better target antigens to elicit protective CD8 responses.

Discussion

Intracellular protozoan parasites possess distinct secretory pathways by which they introduce their proteins into infected host cells, thus providing a means of immune detection by CD8 T cells. The impact of regulated secretion on CD8 T cell responses however, is not known. Here we have identified a relatively ineffective CD8 T cell response in the susceptible (H-2^b) strain of mice that is directed toward a peptide (YAL9) derived from the parasite protein ROP5. ROP5 originates in the rhoptries and is injected directly into the cytoplasm of the host cell during invasion, whereas the highly protective antigen GRA6 is a dense granule protein that is constitutively secreted into the lumen of the parasitophorous vacuole. To test the hypothesis that the mode of protein secretion contributes to the difference in the CD8 response between ROP5 and GRA6, we engineered parasites in which the epitopes from ROP5 and GRA6 were altered in their secretion pattern. Strikingly, parasites in which the ROP5 epitope was secreted via dense granules elicited a much greater

CD8 T cell response, whereas targeting the GRA6 epitope to rhoptries led to decreased responses. Moreover, the combination of immunization of mice with the ROP5 epitope, together with retargeting the ROP5 epitope to dense granules led to strong protection. These data help to unravel the differences between effective versus weak CD8 T cell responses, and have important implications for host-pathogen interactions, and the design of CD8 vaccines to intracellular parasites.

Why does targeting epitopes to dense granules lead to improved CD8 T cell responses? Although we cannot exclude the possibility, this effect is unlikely to be due solely to higher overall levels of the precursor protein, since endogenous ROP5 is already among the most highly expressed proteins in *Toxoplasma* (www.toxodb.org), yet evokes a relatively weak T cell response. In addition, while increased protein levels may contribute to the enhanced CD8 response elicited by the dense-granule targeted GRA6-ROP5, this is not the case for another dense-granule targeted version of the ROP5 epitope, GRA6-YAL9, which is expressed at similar levels to the rhoptry-targeted ROP5 transgene, yet also elicits a stronger response. Moreover, the dense-granule targeted GRA6 protein evokes a substantially higher T cell response compared to the rhoptry-targeted version of the same epitope ROP5-HF10, although both precursor proteins are expressed as similar levels. In addition, since only certain pools of parasite proteins enter host cells and become accessible to the class I MHC processing pathway, there may be little correlation between the amount of precursor protein in the parasite and the number of peptides ultimately displayed on the host cell surface. Lastly, while in some settings there is a correlation between antigen expression levels and the magnitude of CD8 T cell response, this is not always the case. Indeed some studies have revealed little correlation between expression levels of the antigenic precursor protein, the amount of displayed peptide, and the magnitude of CD8 responses (Croft et al., 2013; Dolan et al., 2011; Neefjes et al., 2011; Schwab et al., 2003).

A more likely explanation is that enhanced CD8 recognition is related to the altered spatial and/or temporal pattern of entry of the precursor protein into host cells. For example, whereas rhoptry release provides a single bolus of precursor protein during invasion, constitutive secretion via dense granules may eventually lead to a greater accumulation of the antigenic precursor protein in the infected cell, and ultimately to a higher density of peptide-MHC complexes displayed on the host cell surface.

With regard to the spatial pattern of antigen entry into host cells, at first glance it might be predicted that rhoptry targeting would favor CD8 T cell responses, since parasite proteins are directly secreted into the host cytosol and thus should be able to directly enter the classical MHC-I presentation pathway without crossing a membrane. However, reports of a direct interaction between the parasitophorous vacuole and the host ER could provide an efficient route for cross-presentation of dense granule-targeted antigens (Goldszmid et al., 2009), thus offsetting this potential advantage of rhoptry-targeted antigens.

It is also interesting to consider that rhoptry versus dense granule targeting may also have an impact on the spatial distribution of host cells presenting parasites antigens *in vivo*. This notion stems from the observation that parasites can secrete rhoptry contents into host cells in the absence of productive invasion (Koshy et al., 2010). Indeed, a recent study using

parasites expressing a rhoptry-targeted CRE reporter and mice with a CRE-inducible fluorescent reporter, revealed a much greater number of host cells that had activated the reporter, and thus had received parasite rhoptry proteins, compared to host cells harboring parasites (Koshy et al., 2012). Thus, one could envisage that those CD8 T cell antigens that are targeted for secretion via rhoptries, would be presented more broadly *in vivo*, including on host cells that do not harbor parasites. Such a mechanism could help to explain the poor protection of CD8 T cells directed against rhoptry-derived antigen, since the resulting CD8 effector T cells may be distracted by interacting with non-invaded host cells rather than delivering protective cytokines to infected cells where most needed. Misdirected CD8 effector responses also lead to increased collateral damage by T cells, although the correlation between decreased protection and increased parasite load argues against this as a major mechanism in this setting.

While our data indicate that the mode of secretion has an important impact on CD8 responses, this does not imply that secretion is the sole determinant of antigenicity. Indeed, some parasite antigens derived from dense granule proteins do not trigger strongly immunodominant CD8 T cell responses (Frickel et al., 2008). Other factors, including the route of protein trafficking after secretion, the C-terminal position of the epitope within the source antigen (Feliu et al., 2013), the ability of the peptide to bind MHC, and the affinity and precursor frequency of the responding T cells (Kotturi et al., 2008; Moon et al., 2007; Obar et al., 2008) will undoubtedly have an impact as well. Moreover, while most CD8 T cell responses appear to be targeted to invaded host cells (Goldszmid et al., 2009; Gubbels et al., 2005) the ability of particular antigens to be efficiently cross-presented by non-invaded by-stander cells could potentially promote strong CD8 T cell responses independently of the mode of secretion from the parasite (Mashayekhi et al., 2011).

Apicomplexan parasites, including the disease causing agents *Plasmodium spp.*, *Cryptosporidium*, and *Toxoplasma*, use distinct secretory organelles to deliver parasite effector molecules into the host cells and thereby manipulate host cell physiology. Entry of parasite effector proteins into host cells can potentially alert the host to the presence of an intracellular pathogen, and act as an “Achilles heel” for the parasite. Therefore knowledge of how secretion pattern affects CD8 T cell responses is important to the design of effective vaccines against these agents. In particular, there is intense interest in developing vaccines that elicit CD8 T cell responses to the pre-erthyrocytic form of the malaria parasite, *Plasmodium*. While proteomic and genomic analyses have yielded a large number of possible candidates targets, screening and prioritizing these candidates remains a major challenge (Duffy et al., 2012; Hill, 2011; Vaughan and Kappe, 2012). Our data indicate that determining the mode of secretion of potential vaccine targets may be a powerful approach to narrow down vaccine candidates, and that antigens that reside within parasite dense granules may be particularly promising candidates, whereas rhoptry proteins should be avoided. In addition, our results may aid in the design of more effective vaccine strains of *Toxoplasma gondii*, an approach that is currently being explored to promote anti-tumor immunity (Baird et al., 2013).

Experimental Procedures

Mice

B6.C, C57BL/6 (B6), B10.D2, DBA, CBA, MHC class II - deficient B6.129S-H2$^{dlAb1\text{-}Ea}$ and the TAP deficient B6.129S2-*Tap1*^{tm1Arp}/J mice were obtained from Jackson Laboratory. B6×B6.C (H-2$^{b/d}$), MHC class II deficient B6.129S-H2$^{dlAb1\text{-}Ea}$ and the TAP deficient B6.129S2-*Tap1*^{tm1Arp}/J mice were then bred at UC Berkeley animal facility. H-2^{b} ERAAP deficient mice on C57BL/6 background have been described (Hammer et al., 2006). For all immunization and infection experiments sex and age matched mice were used. Mice were used with the approval of the Animal Care and Use Committee of the University of California.

Generation of transgenic parasites

Transgenic parasites were generated using the type III strain CTGΔ*hxgprt* (Donald et al., 1996), engineered to express luciferase and GFP. “ROP5” construct: DNA sequences encoding ROP5IIC, including its native promoter, were cloned into pHXGPRT adjacent to the *HXPGRT* cassette and in frame with a C-terminal 3× FLAG. “ROP5-HF10” construct: the promoter and coding regions of the type III ROP5C allele were fused to a C-terminal HA-tag and GRA6 epitope HF10 (HPGSVNEFDF). “GRA6” construct: DNA sequences encoding GRA6 type II, including its native promoter and entire coding region, were modified by the addition of a HA epitope between amino acids 50 and 51 of GRA6, and for ‘GRA6-YAL9” construct the last 10 amino acids (HF10) of GRA6 were replaced by the amino acids FAQLSPGQSDYAVANYFFL, where the underlined residues represent the epitope YAL9 from ROP5 type IIC. The “GRA6” construct was also used as the starting plasmid for generation of “GRA6-ROP5” wherein DNA sequences encoding the pseudokinase domain of ROP5 type IIC (Reese et al., 2011) were amplified and cloned downstream of the native GRA6 type II promoter, GRA6 coding sequence up to residue 50, and an in-frame HA tag. The transgenic strains were made by electroporation of linearized plasmids as described (Donald et al., 1996).

In-vivo infection and immunization

Mice were immunized intraperitoneally (i.p.) with 1-5×10^{6} irradiated tachyzoites of the Type II Prugniuad-tomato-OVA strain (Pru) as described (Grover et al., 2012). For inducing protection, mice were immunized in the footpad with activated B6 bone-marrow derived dendritic cells (BMDCs) loaded with synthetic peptide as described (Blanchard et al., 2008). After 7-14 days, mice were given the same dose for boost and then infected 21 days post boost with a lethal dose of live Pru tachyzoites (1×10^{4} - 5×10^{5}) i.p. For chronic infections, mice were orally fed 25-50 cysts of the Pru strains or by i.p. injection of (5×10^{3} - 5×10^{5}) live tachyzoites from parental or transgenic CTG strains. Cysts were obtained from CBA mice infected for 3-5 weeks i.p. with live 400 Pru tachyzoites. Parasite load was analyzed by semi-quantative PCR (Kirisits et al., 2000) or counting individual labeled cysts as described (Grover et al., 2012).

Ex-vivo analysis

Mice were euthanized 3-7 wks post infection or 1-2 wks post immunization. Spleen and brain leukocyte populations were prepared as previously described (Blanchard et al., 2008). The proportion of *T. gondii*-specific or antigen-specific cells was monitored by intracellular cytokine staining (ICCS) for IFN-γ on $CD4^+$ or $CD8\alpha^+$ cells. APCs were either infected the day before or pulsed with antigenic peptide on the same day and were used for the *ex-vivo* IFN-γ assay. Antigen-specific $CD8\alpha^+$cells were also detected via staining using MHC Class I peptide tetramers (see below).

Generation of *Toxoplasma gondii*-specific T cell hybridomas

C57BL/6 mice were immunized with 1×10^6 irradiated Pru tachyzoites (14,000 rads) i.p. Mice were euthanized 7 days post infection and spleens were dissociated into single-cell suspensions. *T. gondii*-specific populations were expanded *in-vitro* by weekly restimulations with irradiated syngeneic splenocytes or irradiated MHC class II-deficient, B6.129S-$H2^{dlAb1\text{-}Ea}$ BMDCs (2000 rads) that were infected with irradiated Pru tachyzoites the day before.

After 8 weeks of *in-vitro* restimulation, T cells were fused to TCRαβ-negative lacZ inducible BWZ.36.CD8α fusion partner, allowing T cell hybridoma activation to be measured by the lacZ response (Malarkannan et al., 2001). The antigen-specificity and MHC-restriction of the hybridomas were assessed by overnight incubation with infected or uninfected BMDCs from wild type C57BL/6 mice in the presence of MHC class I blocking antibodies (Anti-H-$2K^b$ antibody clone: 5F1.5 and anti-H-$2D^b$ antibody clone: B22.249).

Expression cloning

Bacteria were transformed with *T. gondii* cDNA library cloned in pcDNA (Blanchard et al., 2008), and DNA from bacterial transformants (9 cfus / well) was screened to identify the antigen recognized by the T cell hybridoma as described (Blanchard et al., 2008). To further identify antigenic peptides, reverse phase HPLC was used to separate extracts (Blanchard et al., 2008) from COS-7 cells transfected with pTg8E6.1 or pcDNA. 10pmoles of the antigenic peptide, YAL9, was added to the untransfected COS-7 extracts before fractionation. HPLC fractions were collected in 96-well plates, dried and analyzed for antigenicity by the addition of 5×10^4 APCs/well and 1×10^5 T cell hybridoma/well.

In-vitro differentiation and infection

Bone marrow cells, obtained from mouse femurs and tibias, were differentiated into DC's as described (Grover et al., 2012). After differentiation, BMDCs were infected overnight with irradiated tachyzoites (14,000 rads) at various multiplicities of infection (MOI). Next day, cells were washed twice to remove any extracellular parasites and were used in the assays.

Proteasome inhibition

Proteasome inhibitor lactacystin was titrated (10μM to 0μM) onto 96-well plates containing 5×10^4 BMDCs / well in complete RPMI media. Cells were incubated with the inhibitor for 2hrs at 37°C followed by the addition of irradiated tachyzoites. 8hrs post-infection, media

was removed from treated and infected BMDCs and replaced with fresh complete media and the addition of 1×10^5 T cell hybridoma/well.

Flow cytometry

Surface staining with anti-mouse CD4 (RM4-5), CD8α (53-6.7), IFN-γ (XMG1.2) (BD biosciences), anti-mouse KLRG-1 and IL7R (eBiosciences or BioLegend) antibodies was done as per manufacturer's instructions. Intracellular cytokine staining for IFN-γ was performed using the Cytofix/Cytoperm kit (BD Pharmingen). The concentration and time of staining of the fluorescently labeled MHC Class I tetramers bound to *T. gondii* antigenic peptide (NIH Tetramer facility) were optimized and cells were incubated with the tetramer at 4°C for 1hr. The cells were then washed and followed by surface staining at 4°C for 30 min with anti-mouse CD4 or CD8α, B220 (CD45R), KLRG-1 and IL7R antibodies. All flow cytometry data was acquired on an XL Analyzer or FC 500 (Coulter) or BD LSRII and analyzed using FlowJo software (Tree Star).

Western Blotting and Immunofluorescence Analysis

Parasites were harvested from infected HFFs by scraping, passaging through a 27g needle, and filtering through a 5μm filter. They were then washed in PBS, and resuspended in either Laemmli buffer with DTT or NP-40 buffer (25mM Tris, 100mM NaCl, 1mM EDTA, 0.1%NP40 + protease inhibitors). Proteins were separated by 10% SDS-PAGE and transferred to PVDF membrane. Membranes were probed with rat anti-HA antibody directly conjugated to horseradish peroxidase (HRP) (Roche 3F10) or mouse monoclonal (M2) anti-3×FLAG (Sigma), then rabbit anti-SAG1 or rabbit anti-GRA7 and probed with HRP conjugated secondary antibodies. HRP levels were detected by chemiluminescence on film, followed by densitometric analysis (ImageJ, NIH, as described http://howtowesternblot.net/data-analysis-3/quantification/).

For protein localization immunofluorescence of *T. gondii* infected HFF cells was performed as described (Koshy et al., 2012). After membrane permeabilization, HA-tagged proteins were detected by rat anti-HA (Roche) followed by fluorescently conjugated goat anti-rat IgG (Invitrogen). FLAG- tagged proteins were detected with mouse monoclonal (M2) anti-3×FLAG (Sigma) followed by Alexa Fluor 488-conjugated goat anti-mouse IgG (Invitrogen). Rhoptries were marked using mouse anti-ROP2, 3, 4 antibody followed by Alexa Fluor 650-conjugated goat anti-mouse IgG (Invitrogen). Dense granules were marked using rabbit anti-GRA7 followed by Alexa Fluor 650-conjugated goat anti-rabbit IgG (Invitrogen). Images were acquired by standard microscopy at 600× or 1000× magnification with minimal, and equal processing in Image J (NIH).

Statistical analysis

P values were calculated using two-tailed Student's (non-parametric) t-test or 1-way ANOVA with Bonferroni post test in Prism (GraphPad).

Supplementary Material

Refer to Web version on PubMed Central for supplementary material.

Acknowledgments

We are grateful to the NIH Tetramer facility for the YAL9-D^b and the HF10-L^d tetramers and cancer research laboratory flow facility at UC Berkeley. Imaging for immunofluorescence analysis was performed at the Stanford Neuroscience Microscopy Service, supported by NIH NS069375. This research was supported by the National Institutes of Health (PO1AI065831) to Ellen Robey and Nilabh Shastri (R01AI065537) to Ellen Robey, and RO1AI076753 to John Boothroyd. Harshita Satija Grover was supported in part by Cancer Research Coordinating Committee fellowship. Michael L. Reese was supported by an American Cancer Society fellowship. Hamlet Chu was supported by an American Heart Association Postdoctoral Fellowship. Felice Kelly was supported by an NIH F32 fellowship. We thank Jon Boyle for access to unpublished information prior to publication, and Kerry Buchholz for technical assistance and discussion of results.

References

Baird JR, Fox BA, Sanders KL, Lizotte PH, Cubillos-Ruiz JR, Scarlett UK, Rutkowski MR, Conejo-Garcia JR, Fiering S, Bzik DJ. Avirulent Toxoplasma gondii generates therapeutic antitumor immunity by reversing immunosuppression in the ovarian cancer microenvironment. Cancer Res. 2013; 73:3842–3851. [PubMed: 23704211]

Blader IJ, Saeij JP. Communication between Toxoplasma gondii and its host: impact on parasite growth, development, immune evasion, and virulence. Apmis. 2009; 117:458–476. [PubMed: 19400868]

Blanchard N, Gonzalez F, Schaeffer M, Joncker NT, Cheng T, Shastri AJ, Robey EA, Shastri N. Immunodominant, protective response to the parasite Toxoplasma gondii requires antigen processing in the endoplasmic reticulum. Nature immunology. 2008; 9:937–944. [PubMed: 18587399]

Boothroyd JC, Dubremetz JF. Kiss and spit: the dual roles of Toxoplasma rhoptries. Nat Rev Microbiol. 2008; 6:79–88. [PubMed: 18059289]

Brown CR, Hunter CA, Estes RG, Beckmann E, Forman J, David C, Remington JS, McLeod R. Definitive identification of a gene that confers resistance against Toxoplasma cyst burden and encephalitis. Immunology. 1995; 85:419–428. [PubMed: 7558130]

Brown CR, McLeod R. Class I MHC genes and CD8+ T cells determine cyst number in Toxoplasma gondii infection. J Immunol. 1990; 145:3438–3441. [PubMed: 2121825]

Carruthers VB. Host cell invasion by the opportunistic pathogen Toxoplasma gondii. Acta Trop. 2002; 81:111–122. [PubMed: 11801218]

Croft NP, Smith SA, Wong YC, Tan CT, Dudek NL, Flesch IE, Lin LC, Tscharke DC, Purcell AW. Kinetics of antigen expression and epitope presentation during virus infection. PLoS pathogens. 2013; 9:e1003129. [PubMed: 23382674]

Denkers EY, Gazzinelli RT. Regulation and function of T-cell-mediated immunity during Toxoplasma gondii infection. Clin Microbiol Rev. 1998; 11:569–588. [PubMed: 9767056]

Dolan BP, Bennink JR, Yewdell JW. Translating DRiPs: progress in understanding viral and cellular sources of MHC class I peptide ligands. Cell Mol Life Sci. 2011; 68:1481–1489. [PubMed: 21416150]

Donald RG, Carter D, Ullman B, Roos DS. Insertional tagging, cloning, and expression of the Toxoplasma gondii hypoxanthine-xanthineguanine phosphoribosyltransferase gene. Use as a selectable marker for stable transformation. J Biol Chem. 1996; 271:14010–14019. [PubMed: 8662859]

Duffy MF, Selvarajah SA, Josling GA, Petter M. The role of chromatin in Plasmodium gene expression. Cell Microbiol. 2012; 14:819–828. [PubMed: 22360617]

Feliu V, Vasseur V, Grover HS, Chu HH, Brown MJ, Wang J, Boyle JP, Robey EA, Shastri N, Blanchard N. Location of the CD8 T cell epitope within the antigenic precursor determines immunogenicity and protection against the Toxoplasma gondii parasite. PLoS pathogens. 2013; 9:e1003449. [PubMed: 23818852]

Frickel EM, Sahoo N, Hopp J, Gubbels MJ, Craver MP, Knoll LJ, Ploegh HL, Grotenbreg GM. Parasite stage-specific recognition of endogenous Toxoplasma gondii-derived CD8+ T cell epitopes. The Journal of infectious diseases. 2008; 198:1625–1633. [PubMed: 18922097]

Gendrin C, Bittame A, Mercier C, Cesbron-Delauw MF. Post-translational membrane sorting of the Toxoplasma gondii GRA6 protein into the parasite-containing vacuole is driven by its N-terminal domain. International journal for parasitology. 2010; 40:1325–1334. [PubMed: 20420842]

Goldszmid RS, Coppens I, Lev A, Caspar P, Mellman I, Sher A. Host ER-parasitophorous vacuole interaction provides a route of entry for antigen cross-presentation in Toxoplasma gondii-infected dendritic cells. The Journal of experimental medicine. 2009; 206:399–410. [PubMed: 19153244]

Gregg B, Dzierszinski F, Tait E, Jordan KA, Hunter CA, Roos DS. Subcellular antigen location influences T-cell activation during acute infection with Toxoplasma gondii. PLoS One. 2011; 6:e22936. [PubMed: 21829561]

Grover HS, Blanchard N, Gonzalez F, Chan S, Robey EA, Shastri N. The Toxoplasma gondii peptide AS15 elicits CD4 T cells that can control parasite burden. Infection and immunity. 2012; 80:3279–3288. [PubMed: 22778097]

Gubbels MJ, Striepen B, Shastri N, Turkoz M, Robey EA. Class I major histocompatibility complex presentation of antigens that escape from the parasitophorous vacuole of Toxoplasma gondii. Infect Immun. 2005; 73:703–711. [PubMed: 15664908]

Hakim FT, Gazzinelli RT, Denkers E, Hieny S, Shearer GM, Sher A. CD8+ T cells from mice vaccinated against Toxoplasma gondii are cytotoxic for parasite-infected or antigen-pulsed host cells. J Immunol. 1991; 147:2310–2316. [PubMed: 1918963]

Hammer GE, Gonzalez F, Champsaur M, Cado D, Shastri N. The aminopeptidase ERAAP shapes the peptide repertoire displayed by major histocompatibility complex class I molecules. Nat Immunol. 2006; 7:103–112. [PubMed: 16299505]

Hill AV. Vaccines against malaria. Philos Trans R Soc Lond B Biol Sci366. 2011:2806–2814. [PubMed: 21893544]

Holtappels R, Simon CO, Munks MW, Thomas D, Deegen P, Kuhnapfel B, Daubner T, Emde SF, Podlech J, Grzimek NK, et al. Subdominant CD8 T-cell epitopes account for protection against cytomegalovirus independent of immunodomination. Journal of virology. 2008b; 82:5781–5796. [PubMed: 18367531]

Karttunen J, Sanderson S, Shastri N. Detection of rare antigen-presenting cells by the lacZ T-cell activation assay suggests an expression cloning strategy for T-cell antigens. Proc Natl Acad Sci U S A. 1992; 89:6020–6024. [PubMed: 1378619]

Khan IA, Ely KH, Kasper LH. Antigen-specific CD8+ T cell clone protects against acute Toxoplasma gondii infection in mice. J Immunol. 1994; 152:1856–1860. [PubMed: 7907106]

Khan IA, Smith KA, Kasper LH. Induction of antigen-specific parasiticidal cytotoxic T cell splenocytes by a major membrane protein (P30) of Toxoplasma gondii. J Immunol. 1988; 141:3600–3605. [PubMed: 2460541]

Kirisits MJ, Mui E, McLeod R. Measurement of the efficacy of vaccines and antimicrobial therapy against infection with Toxoplasma gondii. International journal for parasitology. 2000; 30:149–155. [PubMed: 10704598]

Koshy AA, Dietrich HK, Christian DA, Melehani JH, Shastri AJ, Hunter CA, Boothroyd JC. Toxoplasma co-opts host cells it does not invade. PLoS pathogens. 2012; 8:e1002825. [PubMed: 22910631]

Koshy AA, Fouts AE, Lodoen MB, Alkan O, Blau HM, Boothroyd JC. Toxoplasma secreting Cre recombinase for analysis of host-parasite interactions. Nat Methods. 2010; 7:307–309. [PubMed: 20208532]

Kotturi MF, Scott I, Wolfe T, Peters B, Sidney J, Cheroutre H, von Herrath MG, Buchmeier MJ, Grey H, Sette A. Naive precursor frequencies and MHC binding rather than the degree of epitope diversity shape CD8+ T cell immunodominance. Journal of immunology. 2008; 181:2124–2133.

Lindberg RE, Frenkel JK. Toxoplasmosis in nude mice. J Parasitol. 1977; 63:219–221. [PubMed: 859079]

Malarkannan S, Mendoza LM, Shastri N. Generation of antigen-specific, lacZ-inducible T-cell hybrids. Methods Mol Biol. 2001; 156:265–272. [PubMed: 11068767]

Mashayekhi M, Sandau MM, Dunay IR, Frickel EM, Khan A, Goldszmid RS, Sher A, Ploegh HL, Murphy TL, Sibley LD, et al. CD8alpha(+) dendritic cells are the critical source of interleukin-12

that controls acute infection by Toxoplasma gondii tachyzoites. Immunity. 2011; 35:249–259. [PubMed: 21867928]

Montoya JG, Liesenfeld O. Toxoplasmosis. Lancet. 2004; 363:1965–1976. [PubMed: 15194258]

Moon JJ, Chu HH, Pepper M, McSorley SJ, Jameson SC, Kedl RM, Jenkins MK. Naive CD4(+) T cell frequency varies for different epitopes and predicts repertoire diversity and response magnitude. Immunity. 2007; 27:203–213. [PubMed: 17707129]

Neefjes J, Jongsma ML, Paul P, Bakke O. Towards a systems understanding of MHC class I and MHC class II antigen presentation. Nature reviews Immunology. 2011; 11:823–836.

Obar JJ, Khanna KM, Lefrancois L. Endogenous naive CD8+ T cell precursor frequency regulates primary and memory responses to infection. Immunity. 2008; 28:859–869. [PubMed: 18499487]

Reese ML, Zeiner GM, Saeij JP, Boothroyd JC, Boyle JP. Polymorphic family of injected pseudokinases is paramount in Toxoplasma virulence. Proceedings of the National Academy of Sciences of the United States of America. 2011; 108:9625–9630. [PubMed: 21436047]

Sanderson S, Shastri N. LacZ inducible, antigen/MHC-specific T cell hybrids. Int Immunol. 1994; 6:369–376. [PubMed: 8186188]

Schaeffer M, Han SJ, Chtanova T, van Dooren GG, Herzmark P, Chen Y, Roysam B, Striepen B, Robey EA. Dynamic imaging of T cell-parasite interactions in the brains of mice chronically infected with Toxoplasma gondii. Journal of immunology. 2009; 182:6379–6393.

Schwab SR, Li KC, Kang C, Shastri N. Constitutive display of cryptic translation products by MHC class I molecules. Science. 2003; 301:1367–1371. [PubMed: 12958358]

Serwold T, Gaw S, Shastri N. ER aminopeptidases generate a unique pool of peptides for MHC class I molecules. Nat Immunol. 2001; 2:644–651. [PubMed: 11429550]

Shen H, Miller JF, Fan X, Kolwyck D, Ahmed R, Harty JT. Compartmentalization of bacterial antigens: differential effects on priming of CD8 T cells and protective immunity. Cell. 1998; 92:535–545. [PubMed: 9491894]

Suzuki Y, Joh K, Kwon OC, Yang Q, Conley FK, Remington JS. MHC class I gene(s) in the D/L region but not the TNF-alpha gene determines development of toxoplasmic encephalitis in mice. J Immunol. 1994; 153:4649–4654. [PubMed: 7963536]

Suzuki Y, Joh K, Orellana MA, Conley FK, Remington JS. A gene(s) within the H-2D region determines the development of toxoplasmic encephalitis in mice. Immunology. 1991; 74:732–739. [PubMed: 1783431]

Vaughan AM, Kappe SH. Malaria vaccine development: persistent challenges. Current opinion in immunology. 2012; 24:324–331. [PubMed: 22521906]

Wilson DC, Grotenbreg GM, Liu K, Zhao Y, Frickel EM, Gubbels MJ, Ploegh HL, Yap GS. Differential regulation of effector- and central-memory responses to Toxoplasma gondii Infection by IL-12 revealed by tracking of Tgd057-specific CD8+ T cells. PLoS pathogens. 2010; 6:e1000815. [PubMed: 20333242]

Highlights

- Different natural CD8 antigens dominate in susceptible versus resistant mouse strains.
- Altering the secretion pattern of antigens alters the magnitude of the T cell response.
- Altered secretion leads to enhanced CD8 effector responses during chronic infection.
- Secretory pathways are key to vaccine design for intracellular parasites.

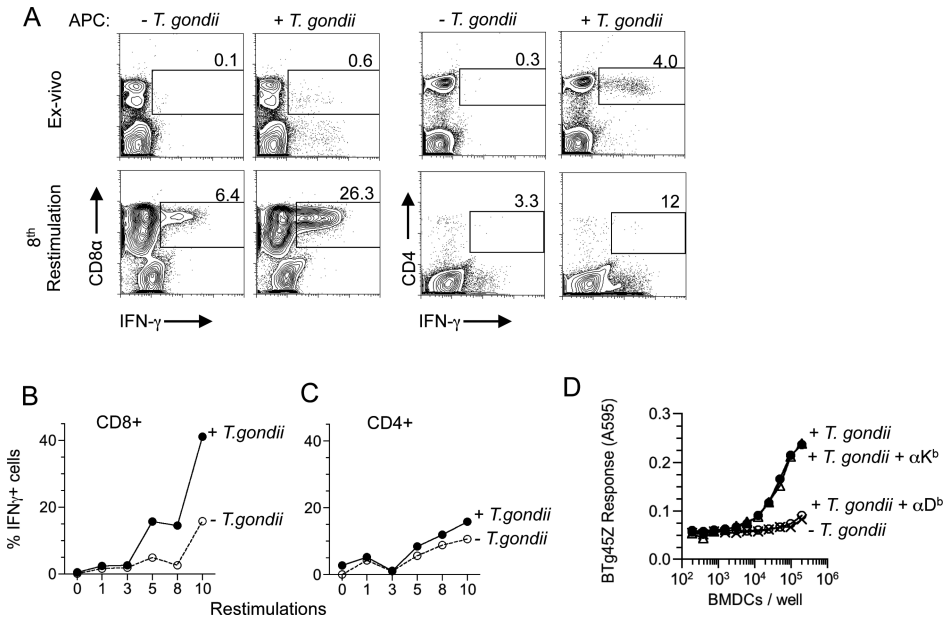

Figure 1. *T. gondii*-specific CD8 T cell responses in B6 mice *ex vivo* and after *in vitro* expansion

C57BL/6 mice were immunized with irradiated *T. gondii* tachyzoites. Splenocytes were harvested from mice 2 wks post immunization and *T. gondii*-specific CD8 and CD4 T cell responses were measured by intracellular cytokine staining for IFN-γ. APCs +/- *T. gondii* were used as stimulators for *ex-vivo* and *in vitro* restimulations. *Ex-vivo* and *in-vitro* restimulation results are shown as **A)** Representative flow cytometry plots **B and C)** Plots depicting the expansion of **B)** CD8 T cells **C)** and CD4 T cells over the course of ten *in-vitro* restimulations. Data are representative of three experiments. **D)** LacZ response of sub-cloned CD8 hybridoma (BTg45Z) after an overnight culture with wild-type APCs +/- *T. gondii* or APCs blocked with antibodies against H-2K^b or H-2D^b MHC I molecules + *T. gondii*. Data is representative of at least two independent experiments.

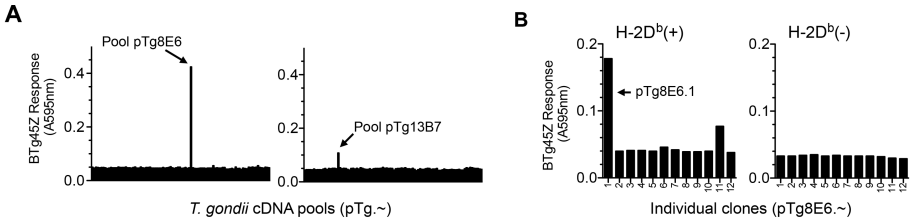

C

TGMe49_108080 (ROP5IIC, Rhoptry kinase family protein 5, IIC)

```
ROP5TypeIIA      MATKLARLATWLVLVGCLLWRAGAVQLSPPNSRTNDLASGTPHVARGDTEAQSGTGDDSD 60
ROP5TypeIIC      MATKLARLATWLVLVGCLLWRAGAVQLSPPNSRTNDLASGTPHVARGDTEAQSGTGDDSD 60
pTg13B7          MATKLARLATWLVLVGCLLWRAGAVQLSPPNSRTNDLASGTPHVARGDTEAQSGTGDDSD 60
pTg8E6.1         ------------------------------------------------------------

ROP5TypeIIA      FPQGVVEEVADMSGGRVPRVPASSTTTSASEGIFRRLVRRLRRGRGTADGAGVADETHQG 120
ROP5TypeIIC      FPQGVVEEVADMSGGRVPRVPASSTTTSASEGIFRRLVRRLRRGRGTADGAGVADETHQG 120
pTg13B7          FPQGVVEEVADMSGGRVPRVPASSTTTSASEGIFRRLVRRLRRGRGTADGAGVADETHQG 120
pTg8E6.1         ------------------------------------------------------------

ROP5TypeIIA      PRPPLRKRLAQHFRRLRGFFGRLTPRWLSGLGRRAQRWWRGRQRPLLDPSFHGLEAGDSF 180
ROP5TypeIIC      PRPPLRKRLAQHFRRLRGFFGRLTPRWLSGLGRRAQRWWRGRQRPLLDPSFHGLEAGDSF 180
pTg13B7          PRPPLRKRLAQHFRRLRGFFGRLTPRWLSGLGRRAQRWWRGRQRPLLDPSFHGLEAGDSF 180
pTg8E6.1         ------------------------------------------------------------

ROP5TypeIIA      MRDLLKHEKELIGYCREEALKEPAAMVEAVMATVWPQNAETTVDSLLSQGERKLKLVEPL 240
ROP5TypeIIC      MRDLLKREEELIGYCREEALKEPAAMVEAVMATVWPQNAETTVDSLLSQGERKLKLVEPL 240
pTg13B7          MRDLLKREEELIGYCREEALKEPAAMVEAVMATVWPQNAETTVDSLLSQGERKLKLVEPL 240
pTg8E6.1         -------------------------------------------VDSLLSQGERKLKLVEPL 18
                                                             ******************

ROP5TypeIIA      RVGDRSVVFLVRDVERLEYFALKVFTMGAENSRSELERLHEATFAAARLLGESPEEARDR 300
ROP5TypeIIC      RVGDRSVVFLVRDVERLEDFALKVFTMGAENSRSELERLHEATFAAARLLGESPEEARDR 300
pTg13B7          RVGDRSVVFLVRDVERLEDFALKVFTMGAENSRSELERLHEATFAAARLLGESPEEARDR 300
pTg8E6.1         RVGDRSVVFLVRDVERLEDFALKVFTMGAENSRSELERLHEATFAAARLLGESPEEARDR 78
                 ****************** ****************************************

ROP5TypeIIA      RRLLLPSDAVAVQSQPPFAQLSPGQSDYAVANYFLLMPAASVDLELLFRTLDFVYVFRGE 360
ROP5TypeIIC      RRLLLPSDAVAVQSQPPFAQLSPGQSDYAVANYFFLMPAASVDLELLFRTLDFVYVFRGE 360
pTg13B7          RRLLLPSDAVAVQSQPPFAQLSPGQSDYAVANYFFLMPAASVDLELLFRTLDFVYVFRGE 360
pTg8E6.1         RRLLLPSDAVAVQSQPPFAQLSPGQSDYAVANYFFLMPAASVDLELLFRTLDFVYVFRGE 138
                 ***********************************:************************

ROP5TypeIIA      EGILARHLLTAQLIRLAANLQSKGLVHGRFTPDNLFLMGYGPVMLGDASALWKVGTRGPA 420
ROP5TypeIIC      EGILARHLLTAQLIRLAANLQSKGLVHGRFTPENLFIMPDGRLMMGDVSTLRKVGTRGPA 420
pTg13B7          EGILARHLLTAQLIRLAANLQSKGLVHGRFTPENLFIMPDGRLMMGDVSTLRKVGTRGPA 420
pTg8E6.1         EGILARHLLTAQLIRLAANLQSKGLVHGRFTPENLFIMPDGRLMMGDVSTLRKVGTRGPA 198
                 ********************************:***:*  * :*:**.*:* ********

ROP5TypeIIA      SSVPVTYAPREFLNANTATFTHALNAWQLGLSIYRVWCLVLPFGLVTPGIKRTWKRPSLR 480
ROP5TypeIIC      SSVPVTYAPREFLNANTATFTHALNAWQLGLSIYRVWCLVLPFGLVTPGIKRTWKRPSLR 480
pTg13B7          SSVPVTYAPREFLNANTATFTHALNAWQLGLSIYRVWCLVLPFGLVTPGIKRTWKRPSLR 480
pTg8E6.1         SSVPVTYAPREFLNANTATFTHALNAWQLGLSIYRVWCLVLPFGLVTPGIKRTWKRPSLR 258
                 ************************************************************

ROP5TypeIIA      VPGTDSLLFDSCIPVPDFVQTLTRRFLNFDRRRRLLPLEAMETPEFLQLQNEISSSLSTG 540
ROP5TypeIIC      VPGTDSLLFDSCIPVPDFVQTLTRRFLNFDRRRRLLPLEAMETPEFLQLQNEISSSLSTG 540
pTg13B7          VPGTDSLLFDSCIPVPDFVQTLTRRFLNFDRRRRLLPLEAMETPEFLQLQNEISSSLSTG 540
pTg8E6.1         VPGTDSLLFDSCIPVPDFVQTLTRRFLNFDRRRRLLPLEAMETPEFLQLQNEISSSLSTG 318
                 ************************************************************

ROP5TypeIIA      QPTAAPSVA 549
ROP5TypeIIC      QPTAAPSVA 549
pTg13B7          QPTAAPSVA 549
pTg8E6.1         QPTAAPSVA 327
                 *********
```

Figure 2. BTg45Z hybridoma recognizes the ROP5 rhoptry protein

A) *T. gondii* cDNA library was screened to identify the antigen recognized by BTg45Z. Two cDNA pools (pTg8E6 and pTg13B7) stimulated the lacZ response of the hybrid. **B)** pTg8E6 was further fractionated to identify a positive cDNA clone pTg8E6.1. BTg45Z response to pTg8E6.1 was antigen-specific and MHC restricted. **C)** *T. gondii* database (www.toxodb.org) BLAST search results revealed that the antigenic cDNA clone pTg8E6.1 encoded a truncated version of the *T. gondii* protein, TGMe49_018080 (Rhoptry kinase family protein 5). Alignment of the amino acid sequence encoded by the truncated cDNA

clone, pTg8E6.1 as compared to the full-length polymorphic clones ROP5IIA and ROP5IIC (Reese et al.) and pTg13B7 is depicted here. (-) represent missing amino acids in the sequence, (*) represent alignment and (: or gap) represents alignment between ROP5IIC and pTg8E6.1 and pTg13B7. See also Figure S1.

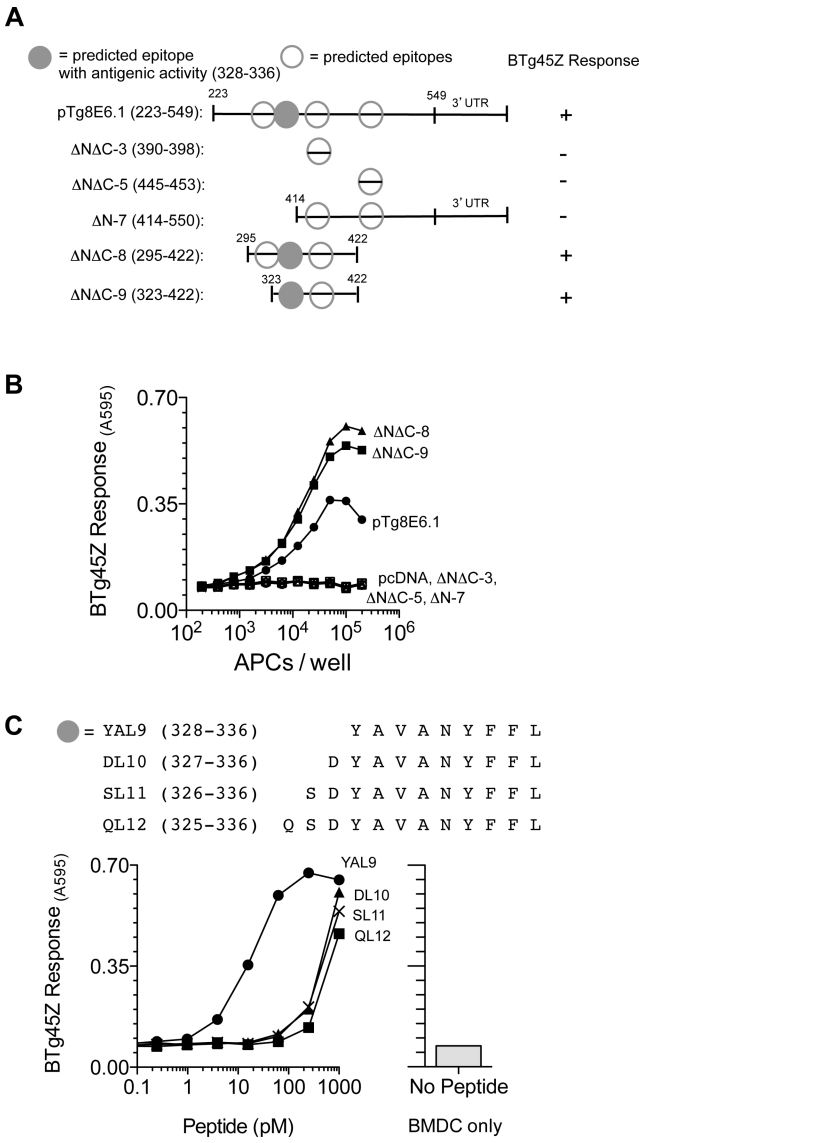

Figure 3. Identification of the antigenic epitope within ROP5IIC that stimulates BTg45Z hybridoma

A) Schematic representation of the N-terminal and C-terminal deletion constructs generated to identify the antigenic epitope within clone pTg8E6.1. The clone was truncated and missing the 5'UTR and nucleotides encoding the first 222 amino acids. The specific amino acids tested in each construct are shown in parentheses and the antigenic activity region is indicated by the filled gray circle. Open circles represent other putative H-2D^b binding epitopes as predicted by the immune epitope database (www.immuneepitope.org) **B)** BTg45Z lacZ response after an overnight stimulation to different deletion constructs that were transfected in H-2D^b expressing APCs **C)** Sequences of antigenic peptide and its N-terminal extended versions. BTg45Z lacZ response to BMDCs alone or BMDCs that were pulsed with varying concentrations of indicated peptides. See also Figures S2 and S3.

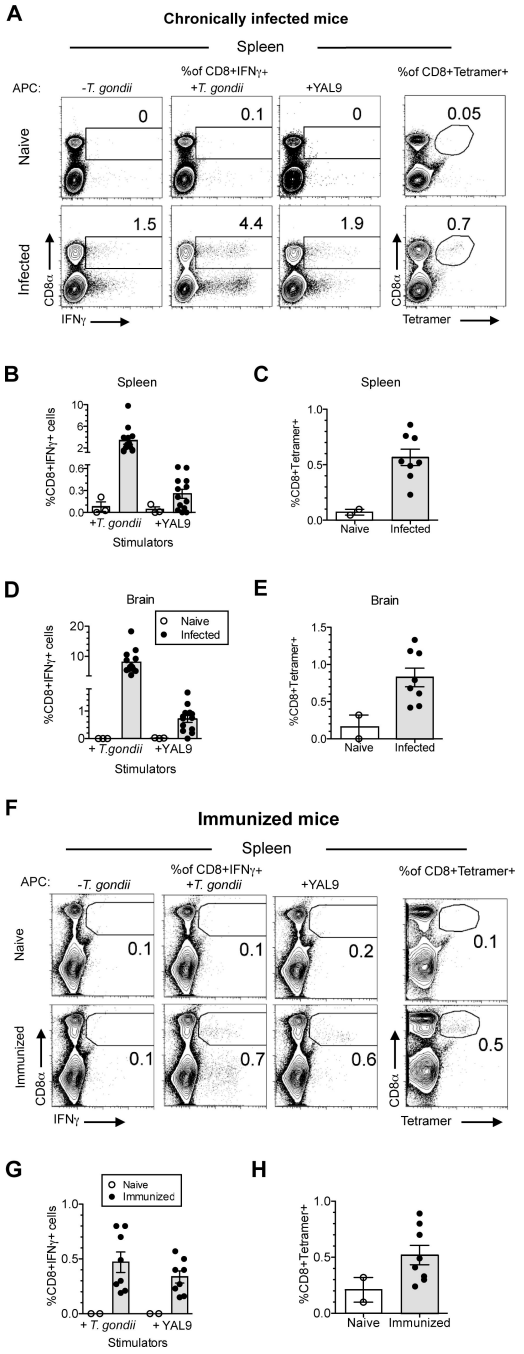

Figure 4. YAL9-specific CD8 T cell response constitutes a detectable fraction of the *in vivo T. gondii*-specific response

A-E) Mice were orally infected with 25-40 *T. gondii* cysts or **F-H)** immunized with irradiated 5×10^6 *T. gondii*, ME49 tachyzoites. Splenocytes and brain leukocytes were harvested from mice 3-4 wks after oral infection or 2 wks after immunization. *T. gondii*-specific T cell responses were measured by intracellular cytokine staining for IFN-γ or by staining with peptide-MHC tetramers. **A)** Representative flow cytometry plots of splenocytes from naïve and infected mice. Left panels show intracellular IFN-γ staining after *in vitro* restimulation with antigen presenting cells either, +/- *T. gondii*, or 1μM YAL9

peptide. Right panels show MHC class I H-2D^b–YAL9 tetramer staining. **B, D)** Compiled data showing *T. gondii*-specific and H-2D^b–YAL9-specific responses from **B)** spleen and **D)** brain of infected mice. Data are corrected for background based on responses by CD8 T cells towards uninfected APCs or APCs pulsed with irrelevant peptide. Each dot represents an individual mouse. **C, E)** Compiled data showing flow cytometry analysis of MHC class I H-2D^b–YAL9 tetramer staining on **C)** splenocytes and **E)** brain leukocytes. Cells were also co-stained with CD8 antibody. **F)** Representative flow cytometry plots of splenocytes from naïve and immunized mice. Left panels show intracellular IFN-γ staining after *in vitro* restimulation with antigen presenting cells either, +/- *T. gondii*, or 1μM YAL9 peptide. Right panels show MHC class I H-2D^b–YAL9 tetramer staining. **G)** Compiled data showing splenic *T. gondii*-specific and H-2D^b–YAL9-specific responses from immunized mice. Data are corrected for background based on responses by CD8 T cells towards uninfected APCs or APCs pulsed with irrelevant peptide. Each dot represents an individual mouse. **H)** Compiled data showing MHC class I H-2D^b–YAL9 tetramer staining on splenocytes from immunized mice. Cells were also co-stained with CD8 antibody. Data are representative of at least three independent experiments. See also Figure S3.

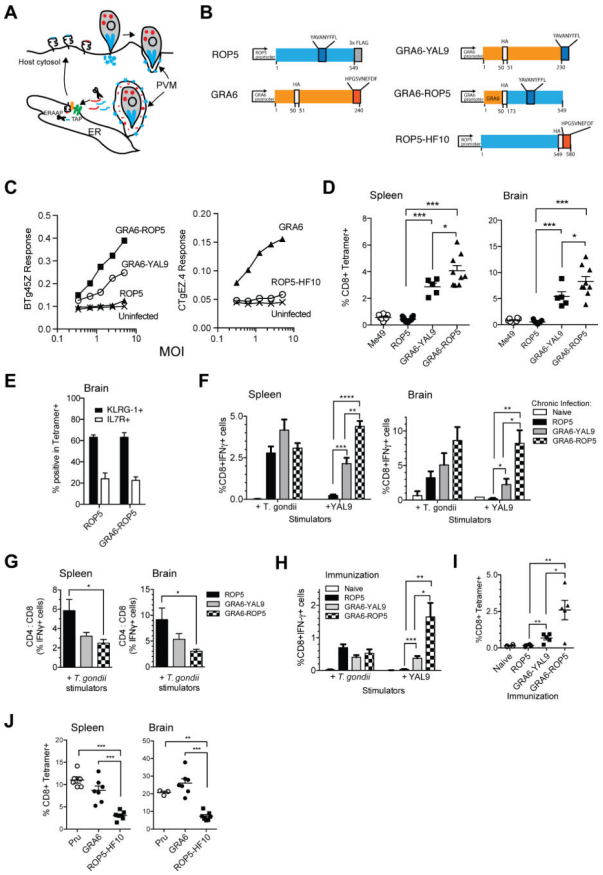

Figure 5. Enhanced T cell response when the antigenic precursor proteins are targeted to parasite dense granules

A) Schematic depicting distinct modes of secretion for the dense granule protein GRA6 (depicted in red) (Holtappels et al., 2008), versus rhoptry protein ROP5 (depicted in blue). Also shown are possible routes for antigen processing and presentation via MHC-I. *T. gondii* injects rhoptry proteins directly into the host cell during invasion. ROP5 associates with the cytosolic face of parasitophorous vacuole membrane (PVM) following secretion. Parasites constitutively secrete dense granule proteins into the PV lumen of invaded host cells. Proteolytic processing of parasite secretory proteins could take place in the host cells' cytosol by the proteasome, and further trimming by ERAAP may occur after TAP-mediated transport of peptides into the ER. Processed peptides are loaded onto MHC class I molecules to be transported to the cell surface for recognition by a CD8 T cell (not depicted). **B)** Left hand diagrams show wild type ROP5 and GRA6 genes indicating the location of their antigenic epitopes (YAL9 and HF10) and placement of HA and FLAG epitope tags. Right hand diagrams show the transgenic constructs used to retarget expression of the epitopes to different parasite secretory compartments. GRA6-YAL9 has the HF10 epitope of the GRA6 gene replaced by YAL9. An additional 10 amino acids from ROP5 flanking the YAL9 epitope were included to allow for efficient processing (not depicted). GRA6-ROP5 contains the GRA6 promoter and signal sequence fused to the C-terminal portion of the ROP5IIC gene including the YAL9 epitope. ROP5-HF10 contains the HF10 epitope from GRA6 fused to the C-terminus of ROP5IIIC gene. All constructs were introduced as transgenes into the

parental type III strain, CTG, which harbors allelic forms of ROP5 and GRA6 that lack the T cell stimulatory epitopes. **C)** BMDCs from C57BL/6 (H-2^b) or B10.D2 (H-2^d) mice were infected *in vitro* with irradiated transgenic *T. gondii* tachyzoites at varying MOI and BTg45Z and CTgEZ.4 lacZ response was measured after an overnight stimulation with BMDCs +/- *T. gondii*. **D)** C57BL/6 mice (H-2^b) were infected i.p. with 10^5 transgenic *T. gondii* tachyzoites. Splenocytes or brain leukocytes were harvested from mice 3-4 wks post infection and *T. gondii*-specific T cell responses were measured by staining with tetramers. Compiled data showing MHC class I H-$2D^b$–YAL9 tetramer staining on gated CD8+ B220- splenocytes (left panel) and brain leukocytes (right panel). **F)** Compiled data showing splenic (left panel) and brain (right panel) *T. gondii*-specific and H-$2D^b$-YAL9-specific CD8 T cell responses from infected mice as measured by intracellular cytokine staining for IFN-γ. Data are corrected for background based on responses by T cells towards uninfected APCs or APCs pulsed with irrelevant peptide. **G)** Plots depicting the ratio of *T. gondii*-specific CD4 to CD8 T cell response from spleen (left panel) or brain (right panel) of infected mice. **H)** Mice were immunized with irradiated 5×10^6 transgenic *T. gondii* tachyzoites. Splenocytes were harvested from mice 2 wks post immunization and *T. gondii*-specific T cell responses were measured using intracellular IFN-γ staining for. Compiled data showing splenic *T. gondii* and YAL9-specific CD8 T cell responses from immunized mice. Data are corrected for background based on responses by T cells towards uninfected APCs or APCs pulsed with irrelevant peptide. **(I)** Compiled data showing MHC class I H-$2D^b$–YAL9 tetramer staining on splenocytes from immunized mice. Cells were also co-stained with CD8 antibody. Each bar represents an average from six mice. Each dot represents an individual mouse. Data are pooled from two independent experiments. **(J)** B6×B6.C (H-$2^{b/d}$) mice were infected with the indicated transgenic *T. gondii* tachyzoites. Splenocytes or brain leukocytes were harvested from mice 21 days post infection and GRA6-specific T cell responses were measured by staining with H-$2L^d$-HF10 tetramers. Compiled tetramer staining data on gated CD8+ B220- splenocytes (left panel) and CD8+ brain leukocytes (right panel). (*=p<0.05, **=p<0.01, ***=p<0.001,****=p<0.0001). See also Figure S4 and S5.

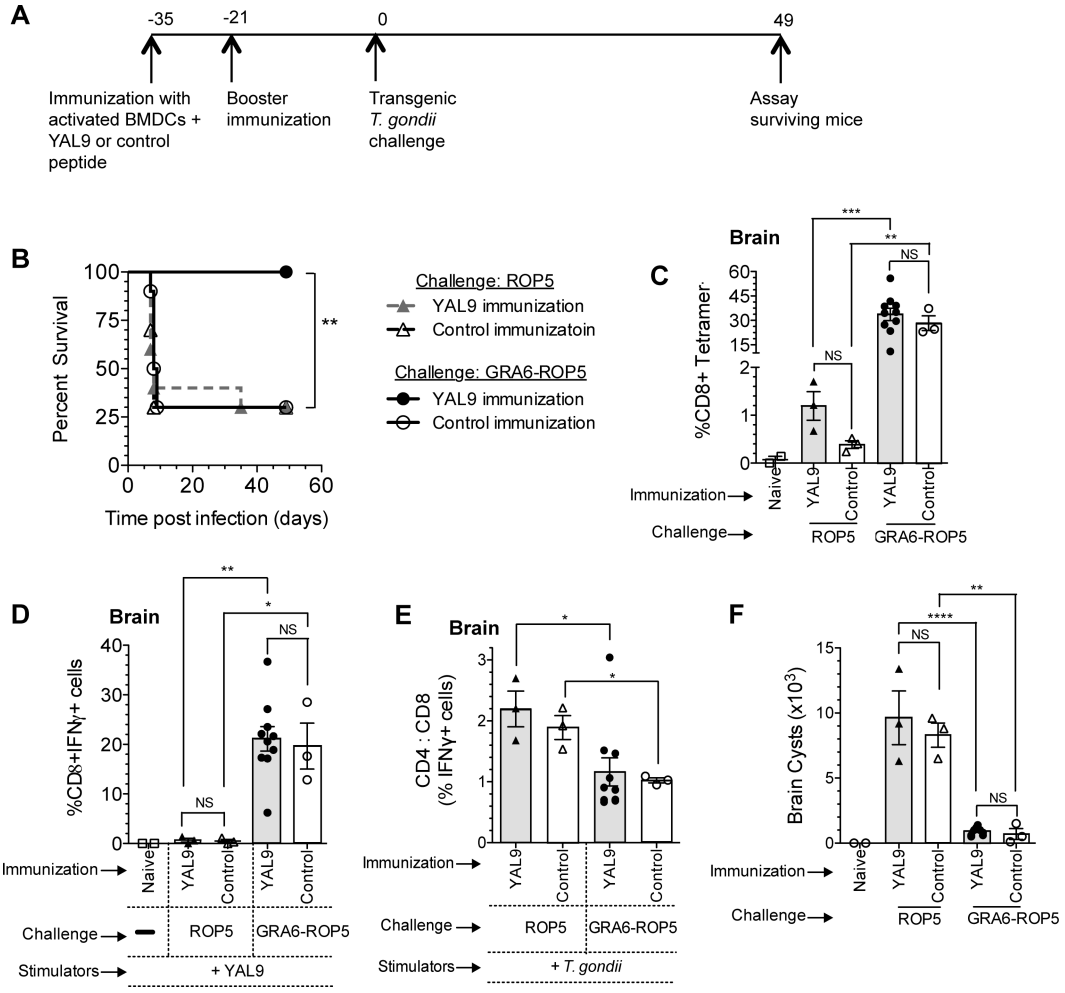

Figure 6. Enhanced protection when the YAL9 epitope is targeted to parasite dense granules

A) Mice were immunized with LPS activated BMDCs pulsed with YAL9 or control peptide (WI9), boosted after 2 wks, and after 3 wks challenged with 5×10^5 live transgenic *T. gondii* tachyzoites i.p. (either CTG+ROP5 or CTG+GRA6-ROP5). **B)** Kaplan-Meier survival curves between the four groups of mice. **C-F)** Mice that survived the acute phase of infection were sacrificed at 7 wks post challenge. **C)** MHC class I H-2D^b–YAL9 tetramer staining on brain leukocytes from surviving mice. Cells were also co-stained with CD8 antibody. **D)** CD8 T cells or **E)** ratio of *T. gondii*-specific CD4 to CD8 T cells in the brain as measured by ICCS for IFN-γ using flow cytometry after *ex-vivo* restimulation with *T. gondii*-infected APCs or peptide-pulsed APCs. Data are background corrected based on the values from uninfected APCs or APC pulsed with irrelevant peptide. **F)** Number of cysts in the brain as measured by staining a portion of the brain with fluorescent lectin to detect the cysts. Data is pooled from two representative experiments with at least 5 mice per condition in each experiment. (*=p<0.05, **=p<0.01, ***=p<0.001, ****=p<0.0001, NS = not significant). See also Figure S6.

Table 1

Oligonucleotide primers for ROP5 deletion constructs

Construct	Forward (5'-3')	Reverse (5'-3')
ΔNΔC-3	GATCCATGTTCACACCTGAAAACCTTTTCATTATGTGAT	CTAGATCACATAATGAAAAGGTTTTCAGGTGTGAACATG
ΔNΔC-5	GATCCATGAATGCGTGGCAACTGGGTCTTAGCATATGAT	CTAGATCATATGCTAAGACCCAGTTGCCACGCATTCATG
ΔN-7	CGCGGATCCGCGATGGTCGGAACCCGAGGACCG	GCTCTAGAGCAGCGACTGAGGGCGCAGC
ΔNΔC-8	CGCGGATCCGCGATGGAGGAGGCACGG	GCTCTAGAGCGCTTGATGCCGGTCCTCG
ΔNΔC-9	CGCGGATCCGCGATGCCAGGACAGAGC	GCTCTAGAGCGCTTGATGCCGGTCCTCG